JEE Journal of Ecological Engineering

Journal of Ecological Engineering, 2026, 27(4), 335–351
https://doi.org/10.12911/22998993/215456
ISSN 2299–8993, License CC-BY 4.0

Received: 2025.11.30
Accepted: 2026.02.18
Published: 2026.03.01

Nano-engineered zeolite mineral combined with Ca-humate: A hybrid ameliorant to improve soil chemical quality in acid sulfate soils

Eko Hanudin[1*], Makruf Nurudin[1], Lis Noer Aini[2]

[1] Department of Soil Sciences, Faculty of Agriculture, Universitas Gadjah Mada, Jl. Flora Bulaksumur, Yogyakarta 55281, Indonesia
[2] Department of Agrotechnology, Faculty of Agriculture, Universitas Muhammadiyah, Jl. Brawijaya, Kasihan, Bantul, Yogyakarta 55183, Indonesia
* Corresponding author's e-mail: ekohanudin@ugm.ac.id

ABSTRACT

Acid sulfate soils (ASS) are characterized by extreme acidity and high aluminum toxicity, which severely restrict plant growth and nutrient availability. To address these challenges, this study evaluated the effectiveness of nano-engineered zeolite (<100 nm) and calcium humate (Ca-humate) as hybrid soil amendments for chemical remediation of ASS. The nano-zeolite was produced through high-energy ball milling of natural zeolite from Klaten, Central Java, yielding 91.41% of particles smaller than 100 nm. Pot experiments were conducted using acid sulfate soils collected from Segoro Anakan Lagoon, Central Java, Indonesia, following a Completely Randomized Design with two amendment factors: nano-zeolite (6, 12, and 18 t ha^{-1}; equivalent to 14, 28, and 42 g pot^{-1}) and Ca-humate (6.88, 8.6, and 10.32 t ha^{-1}; equivalent to 16, 20, and 24 g pot^{-1}), with untreated pots as the control. Results showed that Segoro Anakan ASS had an extremely acidic pH (3.21), high Al and Na saturation, and low N and P levels. Application of nano-zeolite and Ca-humate significantly increased soil pH, cation exchange capacity (CEC), and base cations (Ca^{2+}, Mg^{2+}, K^{+}, and Na^{+}), while reducing exchangeable Al^{3+}, Fe^{2+}, SO_4^{2-}, and pyrite content. The combined application of 12 t ha^{-1} nano-zeolite and 10.32 t ha^{-1} Ca-humate effectively decreased Al^{3+}, Fe^{2+}, SO_4^{2-}, and pyrite concentration by 59.5%, 42.7%, 79.2%, and 50%, respectively. These improvements are attributed to complementary mechanisms of ion exchange, complexation, and pH buffering. The hybrid use of nano-zeolite and Ca-humate represents a promising amelioration strategy to mitigate Al and Fe toxicity and enhance macronutrient availability in tropical acid sulfate soils.

Keywords: acid sulfate soil, nano-zeolite, Ca-humate, aluminum toxicity, soil amelioration, nutrient dynamics.

INTRODUCTION

Acid sulfate soils (ASS) are a major constraint for agriculture and ecosystem health in many tropical coastal regions because of their innate geochemical instability. Upon drainage or exposure to oxygen, sulfidic layers (pyrite-rich) oxidize, producing sulfuric acid that sharply lowers soil pH and mobilizes toxic metals such as Fe^{2+} and Al^{3+}; the result is strongly reduced plant growth, soil fertility loss, and pollution of adjacent waters (Sulaeman et al., 2024; Johnston et al., 2016). In Indonesia alone, coastal and inland ASSs constitute a large land resource: recent surveys estimate ASS coverage in Kalimantan at ~3.5 Mha and national estimates on the order of several million hectares, underscoring the scale of the problem for food security and land use planning (Sulaeman et al., 2024). The socio-economic importance of these soils (rice paddies, tidal agriculture) makes scalable, effective reclamation technologies an urgent priority (Sulaeman et al., 2024; Sarangi et al., 2022; Shamshuddin et al., 2014).

Conventional amelioration measures, principally liming ($CaCO_3$/$Ca(OH)_2$) or gypsum ($CaSO_4 \cdot 2H_2O$) additions, and water-table control, remain effective for neutralizing acidity but have important limitations: they typically

require very large application rates, act transiently under fluctuating redox regimes, and do not fully prevent remobilization of Fe and Al during drying–rewetting cycles (Shamshuddin et al., 2014). These constraints motivate the development of alternative or synergistic reagents that combine pH buffering with persistent sorption/complexation of problem cations and improved nutrient management.

Natural zeolites, particularly modernite, have long been recognized for high cation exchange capacity (CEC), porous frameworks, and ability to adsorb ammonium and certain metals; these properties make zeolites attractive as soil conditioners and carriers for controlled-release fertilizers (Mondal et al., 2021; Legese et al., 2024; Jarosz et al., 2022; Cataldo et al., 2021). More recently, nanostructuring and surface modification of zeolites (nano-engineered zeolites and zeolite-based nanocomposites) have been shown to increase specific surface area, surface reactivity, and adsorption kinetics, thereby improving their efficacy for pollutant immobilization and nutrient retention (Senilă and Cadar, 2024; Kordala and Wyszkowski, 2024; Sharma et al., 2022).

Humic substances, especially calcium humate (Ca-humate), offer synergistic mechanisms. Ca-humate can act as a local pH buffer, chelate Fe and Al (reducing free ionic toxicity), increase phosphorus availability through complexation and ligand exchange, and stimulate beneficial microbial activity that supports soil recovery (Antu et al., 2025; Kordala and Wyszkowski, 2024; Li et al., 2019; Hriciková et al., 2023). Field and controlled experiments have repeatedly reported that humic amendments improve soil nutrient status, enzymatic activity, and microbial community composition over multi-year applications (Li et al., 2019), though responses vary with soil type and initial chemistry.

The concept of a hybrid ameliorant, combining nano-engineered zeolite with Ca-humate, aims to harness synergistic effects: rapid ion capture and high-capacity exchange by the nano-zeolite, together with the chelating, buffering, and biologically active functions of the humate fraction. In ASS contexts, such a hybrid could simultaneously (a) immobilize released Fe/Al under oxidized conditions, (b) provide a controlled source of Ca to neutralize acidity while limiting rapid leaching, and (c) sustain microbial processes and nutrient cycling that favor long-term recovery (Senilă and Cadar, 2024; Jarosz et al., 2022; Li et al., 2019). Nano-engineering further opens the possibility of tuning particle size and surface chemistry to control sorption/desorption rates (Khan et al., 2021; Sharma et al., 2022).

Despite the clear theoretical promise, experimental assessments of nano-zeolite + Ca-humate hybrids in acid sulfate soils are scarce. Most literature treats zeolites and humic materials separately; few studies quantify combined effects on key ASS chemical indicators (pH, EC, SO_4^{2-}, dissolved Fe, Al^{3+}, Ca^{2+}, K^+, and CEC) (Sulaeman et al., 2024; Johnston and Burton, 2016). Therefore, this study aims to determine the effect of the combination of nano-zeolite with Ca-humate to improve the chemical quality of acid sulfate soil from Segoro Anakan and propose the performance mechanism of both ameliorants in adsorbing or complexing cations/anions to explain the observed improvement in soil chemical quality attributes.

MATERIALS AND METHODS

Geological and geographical conditions

Segoro Anakan Lagoon is located in the southwestern coastal zone of Central Java, within the administrative region of Cilacap Regency (Ardli and Wolff, 2009). Geographically, the lagoon is bordered by the Indian Ocean to the south and the mainland of Java to the north. The site shown in Figure 1 represents the eastern part of the lagoonal complex, characterized by extensive mangrove and tidal flat systems that are seasonally inundated. This geomorphological configuration forms a dynamic estuarine ecosystem influenced by tidal exchanges and sediment influx from several rivers, including the Citanduy and Cimeneng (Hilmi et al., 2021).

Geologically, Segoro Anakan was formed through a combination of tectonic subsidence and Holocene sediment accumulation within the Citanduy–Kroya depression zone (Sari et al., 2016; Rosalina, 2016; Christanto, 2009). The area lies within the southern coastal sedimentary basin of Java, which developed during the Plio–Pleistocene as a result of the interaction between the Java subduction zone and alluvial depositional processes. Continuous sedimentation from upstream catchments, particularly from the Citanduy River, contributes to rapid lagoon infilling and shoreline changes (Cahyo et al., 2024).

Over the past decades, extensive land-use changes in the upper watershed have increased soil erosion and sediment delivery to the lagoon. Consequently, fine-grained sediments and organic-rich deposits accumulate in the lowland mangrove zones, forming potential acid sulfate soils when pyrite-bearing materials are exposed to oxidation (Ardli and Yani, 2020; Ardli et al., 2022). The interaction between geological structure, sedimentary dynamics, and hydrological regimes thus plays a crucial role in shaping the soil chemical properties and the occurrence of acid sulfate conditions in Segoro Anakan.

Soil sampling and chemical quality characterization

The acid sulfate soil samples were collected from the Segoro Anakan region, Cilacap, Central Java, Indonesia, at coordinates approximately 7°42'41.20" S and 108°52'41.37" E (Figure 1). Soil samples for the experiment were taken from the topsoil layer (0–30 cm depth). The samples were air-dried until they reached a moisture content suitable for gentle crushing and sieving through a <2 mm mesh. Subsequently, the soil chemical attributes were analyzed.

The soil's chemical characteristics were analyzed using standard soil analytical procedures. Soil pH was determined using three types of extractants: distilled water (H_2O), 1 N potassium chloride (KCl), and concentrated hydrogen peroxide (H_2O_2) with a soil-to-solution ratio of 1:2.5, and the pH was measured using a calibrated pH meter. Electrical conductivity (EC) was measured in a 1:5 soil-to-water suspension using an EC meter (Eviati et al., 2023). Total soil organic carbon (C-organic) was determined using the loss-on-ignition (LOI) method. The samples were oven-dried at 105 °C to remove moisture and weighed (W105), then combusted in a muffle furnace at 550 °C for 4 hours to obtain the ash weight (W550). The soil organic matter (SOM) content was calculated as SOM (%) = [(W105 – W550)/W105] × 100%, and organic carbon content was derived using the conversion factor C-organic (%) = SOM × 0.58 (Martínez et al., 2018). The total nitrogen (N-total) content was determined using the Kjeldahl method, which quantifies ammonium released after digestion of organic nitrogen compounds (Eviati et al., 2023).

Exchangeable base cations (Ca^{2+}, Mg^{2+}, K^+, and Na^+) and cation exchange capacity (CEC) were analyzed using 1 N unbuffered NH_4Cl extractant (modified from Eviati et al., 2023). Available phosphorus (P-available) was extracted with the Bray-1 solution, reacted with ammonium molybdate and ascorbic acid to form a blue complex, and measured spectrophotometrically at λ = 494 nm (Eviati et al., 2023). Available iron (Fe-available) was extracted with diethylenetriaminepentaacetic acid (DTPA) and quantified using atomic absorption spectrophotometry (AAS). Available sulfate (SO_4^{2-}) was extracted using $Ca(H_2PO_4)_2$ solution and measured spectrophotometrically at λ = 494 nm after addition of $BaCl_2$–Tween reagent (Eviati et al., 2023).

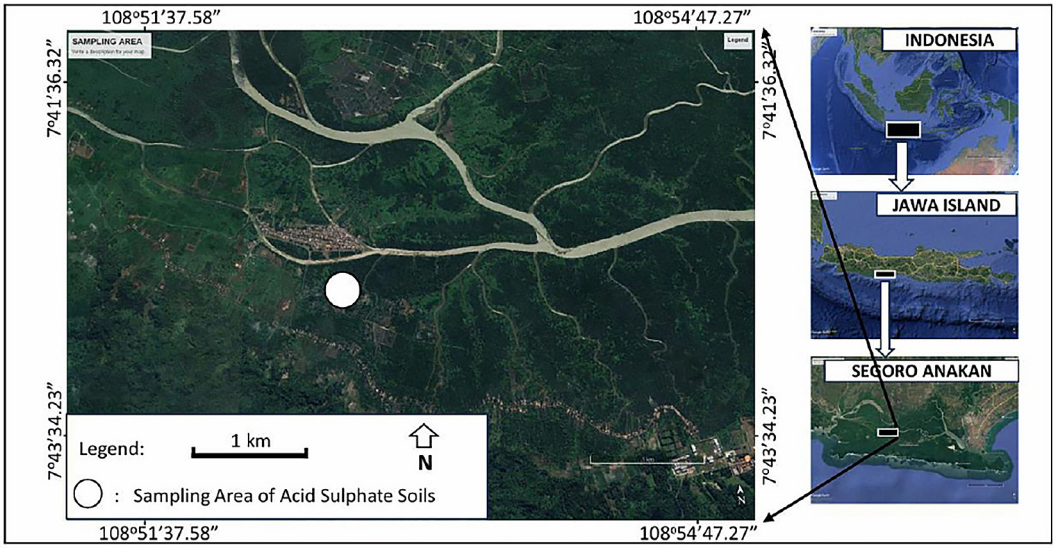

Figure 1. Acid sulfate soil samples collected from a site at Segoro Anakan Area

Exchangeable acidity, comprising exchangeable Al^{3+} and H^+, was determined from a 1 N KCl extract by titration with NaOH (titration I). After precipitation of Al as $Al(OH)_3$, NaF was added, and the solution was back-titrated with HCl (titration II). The Al^{3+} content was calculated from the second titration, while the difference between the two titrations represented exchangeable H^+ (Pansu and Gautheyrou, 2006).

Pyrite (FeS_2) content was analyzed using 1 N KCl and 30% H_2O_2 while heating at 80–90 °C, followed by titration with NaOH (Sabang et al., 2005). The degree of Al saturation (Al_sat), exchangeable sodium percentage (ESP), and sodium adsorption ratio (SAR) were calculated using the following formulas: Al_sat (%) = (Exchangeable Al / CEC) × 100%, ESP (%) = (Exchangeable Na / CEC) × 100%, and SAR = $[Na^+] / \sqrt{((Ca^{2+} + Mg^{2+})/2)}$.

The zeolite used in this study was sourced from Klaten, Central Java, Indonesia, similar to the material used by Kumalasari et al. (2022). The preparation of nano-zeolite followed the high-energy ball milling method described by Subramanian et al. (2015). Zeolite powder (<100 mesh) was ground using steel balls in a planetary ball mill for six hours, producing nanoparticles with a size distribution of which 91.41% were below 100 nm. This mechanical treatment effectively reduces particle size and enhances the surface area and reactivity of the zeolite, thereby increasing its effectiveness in soil amendment applications (Subramanian et al., 2015).

The morphological characterization of the nano-zeolite particles was conducted using a scanning electron microscope (SEM) at various magnifications (Igathinathane et al., 2008). Before imaging, samples were mounted on a double-sided aluminum stub and coated with a 48 nm conductive layer to minimize charging effects during observation. SEM analysis was performed under an accelerating voltage of 22 kV. The resulting micrographs were processed using ImageJ software to determine particle size distribution and morphology. Furthermore, the elemental content of the nano-zeolite particles was analyzed using EDS.

The Ca-humate fertilizer used in this study was obtained commercially and contained 67% CaO, 6% humic acid, and 1% micronutrients. Ca-humate serves as a soil conditioner that can improve cation exchange capacity, enhance nutrient availability, and stabilize soil pH, particularly when combined with zeolite (Deng et al., 2021).

A pot experiment was conducted using a factorial completely randomized design (CRD) with two treatment factors: (i) nano-zeolite applied at three rates (6, 12, and 18 t ha^{-1}; equivalent to 14, 28, and 42 g pot^{-1}), and (ii) Ca-humate applied at three rates (6.88, 8.60, and 10.32 t ha^{-1}; equivalent to 16, 20, and 24 g pot^{-1}). In total, 30 experimental units (pots) were prepared, consisting of the 3 × 3 factorial combinations with three replications, along with three control pots. Each pot contained 10 kg of soil and was incubated for 10 days following amendment application to allow equilibrium reactions between the soil matrix and the added materials. After incubation, soil samples were collected from each pot to evaluate changes in soil chemical properties relative to the initial conditions.

Data from nanoparticle characterization were analyzed using SEM micrographs and quantified via ImageJ software to determine particle size and elemental composition. Statistical analyses were performed using analysis of variance (ANOVA) at a 5% significance level to evaluate the effects of nano-zeolite and Ca-humate treatments. When significant differences were detected, Duncan's multiple range test (DMRT) was employed for mean separation. All statistical analyses were carried out using SAS version 9.1.3, while Pearson's correlation analyses were performed with SPSS version 20.

RESULTS AND DISCUSSION

Soil chemical quality of acid sulfate soil

Based on Table 1, it can be found that the higher pH-H_2O compared to pH-KCl in Segoro Anakan acid sulfate soils results from cation exchange reactions and hydrolysis of exchangeable Al, which releases additional H^+ ions in the KCl medium. The small but negative ΔpH (-0.10) indicates a predominance of weakly negative variable charges typical of Fe- and Al-rich tropical soils. Together with the high Al^{3+} and Fe^{3+} concentrations, these reactions explain the strong acidity and buffering behavior of the soil. Therefore, the relationship pH-H_2O > pH-KCl serves as a diagnostic indicator of exchangeable acidity and proton-generating reactions associated with pyrite oxidation and the abundance of Fe/Al oxides in the acid sulfate soils of Segoro Anakan. The pH-H_2O_2 value of 2.23 confirms the oxidation of

Table 1. Soil chemical quality of acid sulfate soil from Segoro Anakan, Central Java

Soil physico-chemical properties	Value	Grade
pH-H_2O	3.21	Extremely acid
pH-KCl	3.11	
pH-H_2O_2	2.23	
EC ($dS.m^{-1}$)	14.63	Very high
C-org (%)	13.14	Very high
N-Total (%)	0.519	Low
C/N	25.32	High
CEC ($cmol.kg^{-1}$)	21.66	Medium
Available Ca ($cmol.kg^{-1}$)	2.94	Low
Available Mg ($cmol.kg^{-1}$)	0.63	Low
Available K ($cmol.kg^{-1}$)	0.984	High
Available Na ($cmol.kg^{-1}$)	2.88	Very high
Available P ($mg.kg^{-1}$)	3.11	Very low
Fe ($mg.kg^{-1}$)	230.66	Very high
SO_4^{2-} ($mg.kg^{-1}$)	169.26	High
Al-exch. ($cmol.kg^{-1}$)	9.19	Very high
H-exch. ($cmol.kg^{-1}$)	4.18	Very high
Pyrite (%)	0.32	Medium
Al Saturation (%)	42.46	High

pyrite (FeS_2) into sulfuric acid (H_2SO_4), a characteristic process of active acid sulfate soils.

Exposure of pyritic materials in acid sulfate soils (ASS) to aerobic conditions strongly enhances sulfide oxidation and drives severe soil acidification under tropical environments. Fitzpatrick et al. (2017) demonstrated that artificial drainage, tidal-controlled shifts in the water table, and repeated drying–rewetting cycles accelerate pyrite oxidation, producing substantial amounts of acidity that markedly lower soil pH and increase the solubility and mobility of Fe and Al. These processes create highly acidic conditions characteristic of disturbed ASS landscapes. Complementing these mechanistic insights, Sulaeman et al. (2024) reported that coastal ASS in Kalimantan often exhibit extremely low pH values, frequently below 3.5, due to advanced pyrite weathering and the consequent formation of secondary Fe-sulfate minerals such as jarosite [$KFe_3(SO_4)_2(OH)_6$]. The precipitation of jarosite not only reflects intense oxidation of sulfidic materials but also contributes to sustained acidity and continued Fe mobilization within the soil profile. Similar hydrological dynamics occur in the Segoro Anakan mangrove-estuarine system of Cilacap, where periodic tidal inundation, artificial drainage for land conversion, and fluctuating redox regimes similarly promote the oxidation of pyritic sediments, leading to extreme acidity and the development of characteristic acid sulfate soil features.

The very high EC reflects excessive accumulation of soluble salts, primarily Na^+ and SO_4^{2-}, commonly found in coastal acid sulfate soils periodically inundated by seawater (Fitzpatrick et al., 2008). Evaporation of brackish water and limited leaching further concentrate these ions, leading to secondary salinization. The concurrent high Na concentration (2.88 cmol kg^{-1}) indicates incipient sodicity and strong marine influence.

The very high organic carbon content derives from the accumulation of anaerobically decomposed mangrove and wetland sediments, whereas the relatively low total N and high C/N ratio (25.32) indicate slow nitrogen mineralization due to oxygen deficiency and microbial inhibition (Reddy et al., 2023; Sanchez, 2019).

A medium CEC value suggests that both clay minerals and organic colloids contribute to charge balance. However, in strongly acidic environments, surface coatings or precipitates of Fe and Al (oxy)hydroxides may mask or neutralize negative surface charges on soil colloids and reduce measurable CEC, thus abundant organic matter does not always correspond to high CEC (Yin et al., 2023; Sipos et al., 2021)

Exchangeable Ca (2.94 cmol kg^{-1}) and Mg (0.63 cmol kg^{-1}) are low due to intense acidification and leaching processes typical of acid-sulfate soils. Pyrite oxidation generates protons that enhance downward loss of Ca^{2+} and Mg^{2+}, while elevated Al^{3+} and H^+ competitively displace these base cations from exchange sites. This mechanism is well documented in incubation studies on acid-sulfate soils (Azman et al., 2023) and aligns with broader regional assessments showing severe base-cation depletion under strongly acidic tropical conditions (Sulaeman et al., 2024). Potassium (0.984 cmol kg^{-1}) is relatively high, possibly derived from mineral weathering or seawater intrusion, whereas Na (2.88 cmol kg^{-1}) is very high, confirming saline water influence. High Na/Ca ratios may lead to aggregate dispersion, reduced permeability, and poor soil structure (Fitzpatrick et al., 2008).

Available P is very low, primarily due to strong fixation by amorphous Fe and Al oxides in acid sulfate soil environments, where phosphate

is readily bound through sorption and the formation of Fe- and Al-phosphate precipitates (Dhanya and Gladis, 2017). Phosphorus availability declines sharply under highly acidic conditions because elevated Fe^{3+} and Al^{3+} activities promote both intensive sorption and precipitation reactions (Dhanya and Gladis, 2017). The very high Fe (230.66 mg kg^{-1}) and SO_4^{2-} (169.26 mg kg^{-1}) concentrations observed in the soil further indicate intense pyrite oxidation. Fitzpatrick et al. (2008) demonstrated that such oxidation enhances Fe^{3+} and SO_4^{2-} accumulation in soil solution, driving jarosite crystallization and amplifying acid generation.

The extremely high Al-exch (9.19 cmol kg^{-1}) and H-exch (4.18 cmol kg^{-1}) values indicate strong exchangeable acidity due to Al^{3+} hydrolysis. This condition enhances Al toxicity, inhibits root elongation, and limits Ca and Mg uptake (Sanchez, 2019). The pyrite content of 0.32% categorizes this soil as a potential acid sulfate soil (PASS). According to Fitzpatrick et al. (2008), soils containing 0.3–1.0% pyrite can generate substantial acidity when exposed to air. The high Al saturation indicates dominance of acidic cations on exchange sites, leading to nutrient imbalance and base cation deficiency. Reddy et al. (2023) emphasize that Al saturation above 40% severely limits plant growth and nutrient availability.

Nano-zeolite characterization

Natural zeolite taken from the Klaten region, Central Java is categorized as a mordenite type because it has the following characteristics: XRD peaks around $2\theta \approx 9.6°$, 13.5°, 22.2°, 26.7°, which are identical to the JCPDS 29-1257 reference pattern; CEC: 140–160 cmol(+) kg^{-1}; BET surface area: 80–110 $m^2\ g^{-1}$; with SEM it appears to have a fibrous tissue-like morphology and a Si/Al ratio of ±5 (Astuti, et al. 2019; Adila, et al. 2024).

Table 2 shows that after high-energy ball milling, the zeolite particles were successfully reduced to nanoscale dimensions, with 35.61% of particles ranging from 1–10 nm, 24.09% between 10–20 nm, and 31.71% between 20–100 nm. Only a small fraction (6.19%) exceeded 100 nm, while particles larger than 1000 nm accounted for merely 0.02%. The mean particle size of the nano-zeolite was 39.78 nm, indicating a successful nanoscale transformation since more than 90% of the particles were below 100 nm. According to Khan et al. (2017), materials can be categorized as nanostructured when at least 70% of the total particles have dimensions between 1 and 100 nm.

The reduction in particle size can be attributed to repetitive collisions between the zeolite grains and the steel balls during the 6-hour milling process. Thirunavukkarasu and Subramanian (2014) reported that increasing milling duration enhances the fragmentation of mineral particles, producing smaller crystallites and expanding the surface area. The ball milling (up to 6 h) significantly decreases particle size and increases the Brunauer–Emmett–Teller (BET) surface area of zeolites, improving their reactivity and ion-exchange potential. The reduction in particle size enhances the external surface and generates more active sites, which is crucial for catalytic and adsorption applications (Kuznetsov et al., 2025)

The energy dispersive spectroscopy (EDS) results presented in Table 3 and Figure 2 reveal that the nano-zeolite primarily consists of oxygen (56.82%) and silicon (30.71%), with aluminum accounting for 6.89%. Minor elements such as sodium (1.08%), potassium (1.08%), calcium (2.79%), and magnesium (0.62%) are also present. The dominance of Si and Al is characteristic of aluminosilicate frameworks typical of natural mordenite-type zeolites.

Similar elemental compositions were reported by Estiaty (2015), who found that natural zeolites from Indonesia contained Si (72.3%) and Al (10.68%) as major constituents. In a comprehensive review of global natural zeolite deposits, Inglezakis and Zorpas (2012) reported that SiO_2 commonly ranges from approximately 60% to over 80% depending on mineralogical type and degree of alteration, confirming that Si and Al form the tetrahedral framework of natural zeolites. The presence of exchangeable cations such as Na^+,

Table 2. Distribution and percentage of nano-zeolite particle size

Diameter (nm)	Zeolit	
	Amount	%
1–10	1669	35.61
10–20	1129	24.09
20–100	1486	31.71
100–250	290	6.19
250–1000	112	2.40
>1000	1	0.02
Mean = 39.78 nm		

Note: Kumalasari et al., 2021.

Table 3. Elements composition and percentage in nano-zeolite

No	Elements	(%)
1	O	56.82
2	Na	1.08
3	Mg	0.62
4	Al	6.89
5	Si	30.71
6	K	1.08
7	Ca	2.79
8	C	-
9	N	-
10	P	-
11	S	-

Note: Kumalasari et al., 2022.

K^+, Ca^{2+}, and Mg^{2+} serves to balance the negative framework charge generated by Al substitution within the silica lattice, thereby influencing ion-exchange capacity and overall chemical reactivity (Dyer, 2005; Inglezakis and Zorpas, 2012).

The elemental mapping image (Figure 3) shows that silicon is uniformly distributed across the nano-zeolite surface, indicating that the aluminosilicate framework remains structurally intact after ball milling. This pattern is consistent with nanosized zeolite prepared via controlled mechanochemical treatment, where high-energy collisions generate surface defect sites without causing significant disruption of the Si–O–Al backbone (Nassrullah et al., 2022). Such defect formation is known to increase the number of active surface sites and enhance adsorption reactivity.

Moreover, the homogeneous dispersion of Si also reflects the structural integrity typical of mordenite-type zeolites with stable tetrahedral linkages. The absence of elemental segregation suggests that the milling process successfully reduced particle size while maintaining phase uniformity, a feature commonly observed in mechanically activated ZSM-5 and zeolite-Y systems. Recent work by Lima et al. (2024) demonstrated that ball milling can decrease the crystal domain size and increase the external surface area without inducing framework collapse, supporting the interpretation that the nano-zeolite in this study retained its structural coherence after milling.

Alterations in soil acidity, salinity, and reactivity after nano-zeolite-Ca-humate application

Alterations in soil chemical quality after application of hybrid ameliorants are presented in Table 4. The table reveals the mean soil pH-H_2O increased significantly ($P = 0.0024$) from 3.13 in the control to 3.46, 3.53, and 3.61 with the application of 14, 28, and 42 g pot^{-1} nano-zeolite, respectively. Meanwhile, Ca-humate application raised pH-H_2O from 3.21 (16 g pot^{-1}) to 3.54 (24 g pot^{-1}), showing a significant positive effect ($P < 0.05$). In contrast, pH-KCl and pH-H_2O_2 were not significantly affected by nano-zeolite but were improved considerably by Ca-humate ($P < 0.05$). No significant interaction (Z×H) occurred, indicating that both materials worked independently rather than complementarily. The pH enhancement by nano-zeolite can be attributed to its high cation exchange capacity and the ability of its aluminosilicate framework to

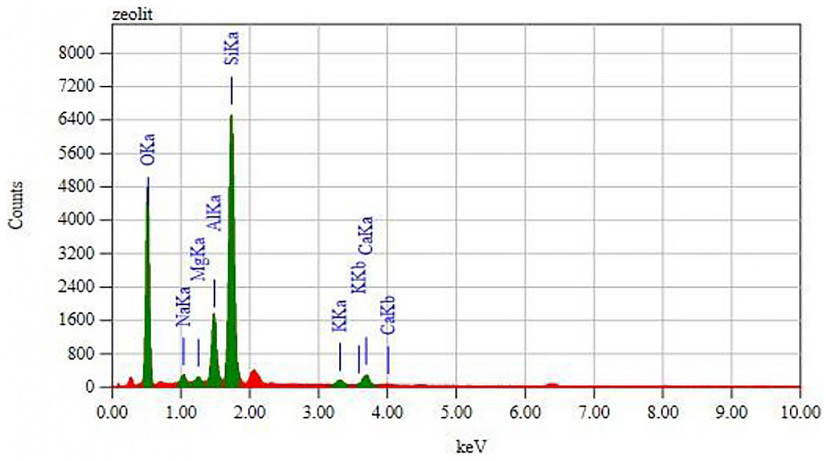

Figure 2. The results of EDS analysis showing the proportion of element content in nano-zeolite (Kumalasari et al., 2021)

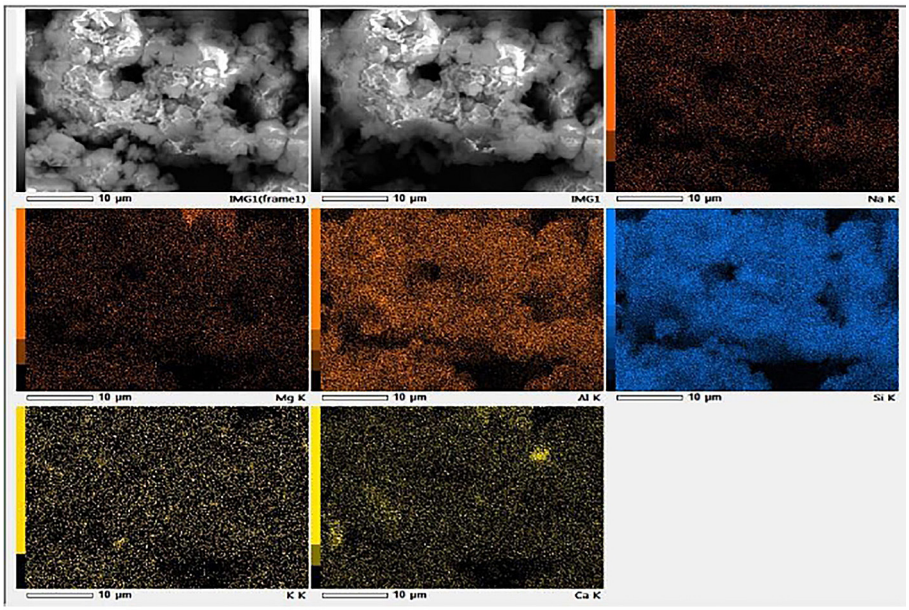

Figure 3. The elemental mapping image demonstrates elements distributed uniformly across the nano-zeolite surface (Kumalasari et al., 2021)

adsorb exchangeable Al^{3+} and H^{+} ions, which are responsible for soil acidity (Mondal et al., 2021). Ca-humate further neutralized acidity through the provision of Ca^{2+} ions and the complexation of Al^{3+} by carboxyl and phenolic groups of humic substances (Maftu'ah et al., 2024).

Nano-zeolite increased EC from 1.26 to 1.39 dS m^{-1}, while Ca-humate raised EC from 1.23 to 1.47 dS m^{-1}, both showing significant main effects ($P < 0.05$). The moderate EC rise reflects enhanced ionic activity driven by the release of exchangeable Ca^{2+}, Mg^{2+}, and K^{+} as nano-zeolite accelerates cation-exchange equilibria, particularly through rapid desorption of surface-bound cations. Ca-humate further contributes by mobilizing base cations via complexation and microaggregate dispersion, increasing the concentration of solvated ions without reaching levels indicative of salinity stress. Consistent with this pattern, Mondal et al. (2021) reported that zeolitic amendments typically raise EC due to intensified ion-exchange dynamics and the expansion of the readily exchangeable cation pool.

Nano-zeolite alone did not significantly affect soil organic carbon (C-Org), which averaged 2.06–2.18%, whereas Ca-humate increased C-Org significantly ($P = 0.001$), ranging from 2.07% at 16 g pot^{-1} to 2.65% at 24 g pot^{-1}. CEC followed a similar trend: nano-zeolite produced a slight but non-significant increase (from 28.18 to 31.45 cmol(+) kg^{-1}), while Ca-humate significantly enhanced CEC (from 30.12 to 36.42 cmol(+) kg^{-1}). The improved CEC reflects the contribution of humic colloids bearing negative functional groups that bind cations reversibly, thus expanding exchange capacity and nutrient retention. Whitton et al. (2023) found comparable improvements in CEC following humate addition, attributing this to enhanced organo-mineral complexation and stabilization of soil organic matter.

Exchangeable Al showed a highly significant decline with nano-zeolite application ($P = 0.009$), dropping from 17.29 cmol(+) kg^{-1} in the control to 11.6 cmol(+) kg^{-1} at 42 g pot^{-1}. Ca-humate had a comparable effect, decreasing Al^{3+} from 16.8 to 10.5 cmol(+) kg^{-1} and reducing Al saturation from 61.32% to 44.27%. The exchangeable H^{+} was not significantly affected by either treatment. These results indicate effective amelioration of Al toxicity by both materials, mainly through ion exchange and complexation processes. Nano-zeolite exchanges Al^{3+} with Ca^{2+} and Na^{+} in its lattice, while Ca-humate complexes Al^{3+} through its carboxyl sites, preventing hydrolysis and acid regeneration. Zeolite reduced Al^{3+} activity primarily through surface adsorption and subsequent surface-precipitation reactions that favour formation/encapsulation into Al-hydroxide phases, thereby lowering soluble Al and exchangeable Al pools in acidic soils (Belviso, 2020).

Pyrite content responded very strongly to both amendments ($P < 0.001$), with a clear Z×H

interaction ($P < 0.001$). The average pyrite content decreased from 0.26% in the control to 0.18% at 28 g pot^{-1} and 0.15% at 42 g pot^{-1} nano-zeolite. Similarly, increasing the Ca-humate dose from 16 to 24 g pot^{-1} reduced pyrite from 0.22% to 0.14%. This substantial decline suggests oxidative transformation of FeS_2 into less reactive Fe(III) compounds such as goethite and ferrihydrite. Humic substances may have accelerated microbial oxidation by serving as electron shuttles, while zeolite improved soil aeration and redox buffering. Whitton et al. (2023) observed comparable processes where humate additions modified microbial–mineral interactions and enhanced Fe–S transformations in anaerobic soils.

Overall, the chemical improvement of acid sulfate soil can be attributed to complementary mechanisms: (i) nano-zeolite increased soil pH and reduced Al^{3+} through cation exchange and adsorption, (ii) Ca-humate improved organic matter content, CEC, and Al complexation, and (iii) both materials jointly promoted Fe–S oxidation that lowered pyrite content. These processes collectively contribute to the rehabilitation of acid sulfate soils by lowering exchangeable acidity and toxic Al levels while improving nutrient retention and buffering capacity.

Integrating nano-zeolite and Ca-humate appears to be an effective strategy for ameliorating acid sulfate soils. The independent yet complementary effects improve soil acidity status, CEC, and reduce Al toxicity and Fe–S mineral instability. Although no strong interaction effect was observed for most parameters, both materials contributed significantly to chemical restoration when applied together. This approach supports sustainable soil management in coastal lowlands where acid sulfate soils constrain agricultural productivity.

Alterations in soil nutrient composition after nano-zeolite-Ca-humate application

Alterations in soil chemical quality concerning the nutrient composition after application of nano-zeolite-Ca-humate are presented in Table 5. The factorial experiment revealed that the application of nano-zeolite (Z) had a significant impact on several soil chemical parameters, whereas Ca-humate (H) alone had limited effects within the applied dosage range. The interaction between Z and H was significant only for Ca availability, indicating a synergistic effect of these amendments on soil cation dynamics. These results suggest that the observed responses are primarily driven by the physicochemical characteristics of nano-zeolite and its interaction with the humic-based organic component.

Nano-zeolite significantly increased total nitrogen (N-tot) and reduced the C/N ratio, reflecting improved nitrogen retention and availability. This aligns with findings by Latifah et al. (2017) and Omar et al. (2020), who demonstrated that clinoptilolite-zeolite-amended urea reduces NH_4^+ and NO_3^- leaching, increases soil

Table 4. Soil acidity, salinity, and reactivity after a hybrid ameliorant application

Treatment	pH- H_2O	pH-KCl	pH- H_2O_2	EC (ds/m)	C-Org (%)	CEC (cmol/kg)	Al-exch (cmol/kg)	H-exch (cmol/kg)	Al Saturation (%)	% Pyrite
Z_0H_0	3.13b	3.09b	2.82b	9.40d	15.13a	28.18b	17.29a	3.63a	28.18b	0.26a
$Z_{14}H_{16}$	3.41a	3.18ab	2.90a	9.77cd	14.79ab	35.71a	11.60ab	3.16a	35.71a	0.15d
$Z_{14}H_{20}$	3.41a	3.25a	2.89ab	10.87abc	14.62ab	33.23ab	9.94b	2.76a	33.23ab	0.18c
$Z_{14}H_{24}$	3.59a	3.15ab	2.89ab	10.17bcd	14.05bc	37.36a	7.63b	3.53a	37.36a	0.16d
$Z_{28}H_{16}$	3.45a	3.24a	2.88ab	10.37abcd	14.15bc	36.71a	9.01b	2.69a	36.71a	0.27a
$Z_{28}H_{20}$	3.44a	3.20ab	2.88ab	11.60a	13.92bc	36.92a	11.61ab	2.58a	36.92a	0.19c
$Z_{28}H_{24}$	3.48a	3.26a	2.90a	11.50a	13.93bc	31.10ab	10.10b	2.30a	31.10ab	0.10f
$Z_{42}H_{16}$	3.47a	3.14ab	2.89ab	10.87abc	13.69c	32.97ab	11.02b	1.46a	32.97ab	0.10f
$Z_{42}H_{20}$	3.52a	3.22a	2.92a	11.30ab	13.98bc	33.53ab	10.25b	1.67a	33.53ab	0.23b
$Z_{42}H_{24}$	3.61a	3.24a	2.94a	11.20ab	13.64c	33.64ab	7.00b	2.26a	33.64ab	0.13e
$Sig.P_{0.05}$										
Z	0.002449**	0.47573	0.57027	0.030213*	0.254379	0.25438	0.00946**	0.5346	0.25438	1.190e-12***
H	0.0134749	0.02952*	0.01307*	0.002066**	0.001015**	0.00101**	0.87878	0.1334	0.00101**	0.6396
Z*H	0.833626	0.15177	0.65871	0.709897	0.595772	0.59577	0.66262	0.9278	0.59577	2.713e-14***

Table 5. Soil nutrient alteration after a hybrid ameliorant application

Treatment	N-tot (%)	C/N	P-avail (mg/kg)	K-avail (cmol/kg)	Ca-avail (cmol/kg)	Na-avail (cmol/kg)	Mg-avail (cmol/kg)	Fe-avail (mg/kg)	SO_4^{2-}-avail (mg/kg)
Z_0H_0	0.61b	24.97a	3.60a	0.67c	4.91d	1.16a	2.58c	29.09a	155.39a
$Z_{14}H_{16}$	0.72ab	20.32ab	6.57a	1.53bc	7.88bc	3.18a	2.90bc	19.70b	73.22ab
$Z_{14}H_{20}$	0.61b	23.90a	7.32a	1.00bc	8.15abc	3.29a	3.06abc	20.49ab	101.89ab
$Z_{14}H_{24}$	0.65ab	21.4ab	4.83a	1.28bc	10.05a	3.31a	3.15ab	17.83b	97.48ab
$Z_{28}H_{16}$	0.60b	24.13a	7.65a	1.75ab	9.79ab	3.63a	3.23ab	18.22b	91.88ab
$Z_{28}H_{20}$	0.61b	22.87ab	6.01a	1.22bc	7.83bc	3.40a	3.00abc	21.83ab	77.84ab
$Z_{28}H_{24}$	0.76a	18.23b	6.29a	1.39bc	8.63abc	3.25a	3.15ab	18.20b	74.47ab
$Z_{42}H_{16}$	0.62b	22.59ab	6.17a	1.25bc	7.49c	3.32a	3.05abc	13.02b	77.78ab
$Z_{42}H_{20}$	0.62b	22.82ab	5.07a	1.45bc	9.39abc	3.57a	3.52a	15.40b	107.26ab
$Z_{42}H_{24}$	0.72ab	18.72b	6.91a	2.40a	7.33c	3.33a	3.00abc	16.68b	32.28b
$Sig.P_{0.05}$									
Z	0.0326*	0.0132 *	0.18767	0.01516*	0.0005543***	2.07e-10 ***	0.0386*	0.0118*	0.107
H	0.9556	0.9167	0.82682	0.15394	0.3775291	0.311	0.5275	0.1293	0.747
Z*H	0.0985.	0.2552	0.46359	0.06477	0.0119316*	0.322	0.1844	0.8494	0.611

Note: "*" significant; "ns" non-significant; Z_0H_0 = No treatment (control);
Z_{14} = 14 g nano-zeolite/pot ≈ 6 ton nano-zeolite/ha;
Z_{28} = 28 g nano-zeolite/pot ≈ 12 ton nano-zeolite/ha ≈; Z_{42} = 42 g nano-zeolite/pot ≈ 18 ton nano-zeolite/ha;
H_{16} = 16 g Ca-humate/pot ≈ 6.88 ton Ca-humate/ha; H_{20} = 20 g Ca-humate/pot ≈ 8.6 ton Ca-humate/ha;
H_{24} = 24 g Ca-humate/pot ≈ 10.32 ton Ca-humate/ha.

total N and exchangeable NH_4^+, and ultimately improves nitrogen use efficiency and crop yield through strong ammonium adsorption and gradual N release from zeolitic surfaces. Zeolitic surfaces with high cation-exchange capacity (CEC) immobilize NH_4^+ ions, reducing volatilization and leaching while promoting gradual nitrogen release (Latifah et al., 2017; Omar et al., 2020), which is consistent with the higher total N and lower C/N ratio observed in zeolite-treated soils compared to the control.

Although phosphorus availability (P-avail) tended to increase in most zeolite treatments, the effect was statistically insignificant ($p > 0.05$). The lack of significance may be attributed to strong Fe–P fixation in these acid soils, where Fe-oxides dominate P binding (Aainaa et al., 2018). Clinoptilolite-based zeolite can act as a slow-release P reservoir, but its effectiveness is strongly controlled by soil pH and the abundance of reactive Fe and Al oxyhydroxides (Hasbullah et al., 2020). Ca-humate may form stable Fe–humate complexes that slightly improve P mobility, but its short-term effect appears limited in this experiment.

Potassium (K-avail), calcium (Ca-avail), magnesium (Mg-avail), and sodium (Na-avail) were significantly affected by nano-zeolite, indicating its dual role as a source and regulator of exchangeable bases. Clinoptilolite-type zeolites typically host Na^+, K^+, Ca^{2+} and Mg^{2+} as framework charge-balancing exchangeable cations, which can be gradually released to and exchanged with the soil solution (Kordala and Wyszkowski, 2024; Javaid et al., 2024; Mondal et al., 2021). The significant increase in Ca-avail and the Z×H interaction suggest a synergistic enhancement, likely due to Ca release from Ca-humate and its stabilization within the zeolite matrix. Similar mineral–organic combinations, where zeolite is combined with mineral fertilizers or organic amendments, have been shown to increase nutrient retention, slow the release of cationic nutrients, and improve soil chemical fertility, including cation exchange-related properties (Legese et al., 2024; Doni et al., 2024; Wang et al., 2025), which is consistent with the trends observed in this study.

Interestingly, Fe-availability decreased significantly with nano-zeolite treatment, which is beneficial for acid sulfate soil remediation. The reduction of Fe^{2+}/Fe^{3+} activity likely results from pH buffering, Ca-induced precipitation of Fe-hydroxides, and Fe–humate complexation. Studies on acid sulfate soils have shown that Ca-based amendments such as calcium silicate combined

with ground magnesium limestone (GML) effectively increase soil pH and reduce exchangeable acidity and toxic metal activity, thereby improving soil chemical conditions (Azman et al., 2023). Similarly, Si-humate formulations containing humic substances, rice husk biochar, and agricultural lime have been demonstrated to enhance soil pH and mitigate the solubility of Fe and sulfate, while alleviating Fe toxicity to rice (Maftu'ah et al., 2024). Although SO_4^{2-} availability decreased in some treatments, the effect was not statistically significant, suggesting that sulfate dynamics require longer-term monitoring to detect stable changes.

Overall, the experimental outcomes emphasize that nano-zeolite acts as the dominant factor in improving soil nutrient status and mitigating Fe toxicity in acid sulfate soils. Ca-humate complements these effects through complexation and stabilization mechanisms but requires prolonged incubation or repeated application to manifest statistically significant impacts. The combined Z×H treatment, particularly at higher dosages, shows promise for sustainable amelioration of tropical acid sulfate soils.

These findings are consistent with contemporary literature highlighting zeolite's multifunctional role as a high-CEC cation exchanger, pH buffer, and nutrient reservoir (Javaid et al., 2024), and the capacity of humic substances to promote organic complexation, nutrient retention, and soil microbial activation (Maffia et al., 2025; Santi et al., 2024). Continued investigation under field-scale and long-term conditions, particularly for zeolite–humic combinations, is recommended to validate these complementary effects and to assess potential shifts in sodium accumulation and sulfate reduction (Li et al., 2025).

Pearson's correlation of the soil chemical quality attributes

Pearson's correlation matrix (Figure 4) provides an integrated overview of the relationships among soil chemical variables affected by the factorial combination of nano-zeolite (14–42 g $pot^{-1} \approx 6–18$ t ha^{-1}) and Ca-humate (16–24 g $pot^{-1} \approx 6.88–10.32$ t ha^{-1}) in acid sulfate soils of Segoro Anakan, Central Java. Several significant correlations reveal coherent geochemical processes influenced by the amendments.

A strong positive correlation was found among EC, Na-available, and SO_4^{2-}, indicating that the ionic conductivity of the soil solution is mainly governed by Na^+ and sulfate accumulation. This pattern reflects the oxidation of pyrite ($FeS_2 \rightarrow Fe^{2+} + SO_4^{2-} + H^+$) and saline intrusion characteristics of coastal acid sulfate soils (Bautista et al., 2023). In contrast, Ca-available, K-available, Mg-available, and N-total showed moderate to strong positive correlations, suggesting that zeolite and Ca-humate application improved base saturation and nutrient retention through ion exchange and CEC enhancement (Mondal et al., 2021; Cataldo et al., 2021).

Fe-available correlated positively with SO_4^{2-} and pyrite but negatively with Ca-available and soil pH, indicating reduced Fe solubility under higher Ca and pH conditions due to $Fe(OH)_3$ precipitation and Fe–humate complexation. Similar mechanisms have been reported in acid sulfate soils where Ca-based amendments increase pH and exchangeable Ca while decreasing soluble Fe through precipitation and stabilization with organic functional groups (Maftu'ah et al., 2024; Maharani et al., 2025). Likewise, Al-exchangeable and Al-saturation declined as soil pH increased, highlighting the acid-driven mobilization of Al and its mitigation through Ca exchange and organo-metal complexation under amended conditions (Gillespie et al., 2021; Lạto et al., 2025).

Organic carbon (Corg) and CEC correlated moderately with nutrient retention variables (N, Ca, K, Mg), confirming the contribution of humic materials to soil buffering capacity. However, correlations with salinity-related variables (Na, SO_4^{2-}) were weak, suggesting that organic inputs alone cannot fully mitigate ionic stress without the mineral component provided by zeolite. The weak or non-significant correlations of P-available with other parameters reflect the complexity of P fixation by Fe/Al oxides under acid sulfate conditions.

In summary, the correlation structure highlights two dominant clusters: (1) the salinity–sulfate group (EC–Na–SO_4) driven by pyrite oxidation and salt accumulation, and (2) the fertility–buffering group (Ca–K–Mg–N–pH–CEC) enhanced by the complementary action of nano-zeolite and Ca-humate. The negative associations of Fe and Al with Ca and pH confirm the ameliorative potential of these amendments in reducing soil acidity and Fe/Al toxicity. These results agree with recent international findings (Bautista et al., 2023; Mondal et al., 2021).

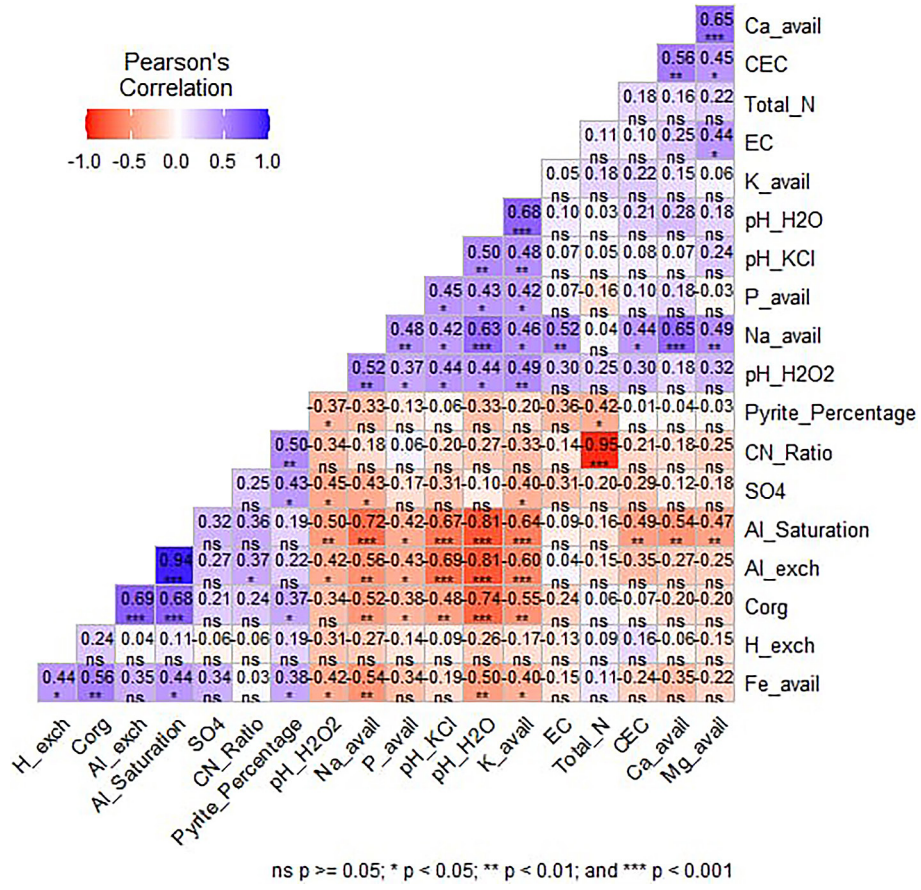

Figure 4. Pearson's correlation describing the relationship among the soil chemical quality attributes of acid sulfate soil ameliorated by nano-zeolite and Ca-humate

Proposed reaction mechanism of nano-zeolite and Ca-humat in altering the chemical quality of acid sulfate soil

Based on the preceding description, both exchangeable Al and Al saturation exhibited a highly significant decrease following the application of nano-zeolite and Ca-humate, whereas exchangeable H^+ was not significantly influenced by either treatment. These findings suggest that both materials effectively ameliorate Al toxicity, primarily through ion exchange and complexation mechanisms. Nano-zeolite facilitates the replacement of Al^{3+} by Ca^{2+} and Na^+ within its crystalline framework, while Ca-humate forms stable complexes with Fe^{3+}/Al^{3+} through carboxyl functional groups, thereby inhibiting hydrolysis and preventing acid regeneration. Similarly, Belviso (2020) reported that zeolite mitigates Al^{3+} activity via surface adsorption and the precipitation of Al-hydroxide polymers.

A notable reduction in Fe availability was observed following the application of nano-zeolite combined with Ca-humate, indicating a promising strategy for improving acid sulfate soil conditions. The lowered activity of Fe^{2+}/Fe^{3+} is largely driven by the enhanced soil pH buffering provided by nano-zeolite and the ability of humic components to strongly bind Fe ions, leading to the formation of stable Fe–humate complexes. This behavior aligns with the conceptual framework presented by Palansooriya et al. (2020), which highlights that reactive mineral surfaces together with organic functional groups can effectively reduce metal mobility via hydroxide formation and organo-metallic complexation. Furthermore, according to Bautista et al. (2023), the association of humic substances with dissolved Fe is a key factor in restricting Fe solubility in acid sulfate environments, reinforcing the complementary role of nano-zeolite and Ca-humate in mitigating Fe transport.

Building on this, our correlation analysis further confirms the geochemical processes underlying Fe mobilization in acid sulfate soils. Fe availability showed a positive correlation with SO_4^{2-} and pyrite contents, but a negative correlation

with soil pH and available Ca, indicating that elevated pH and Ca activity suppress Fe solubility via $Fe(OH)_3$ precipitation and organic complex stabilization. Similar interactions between humic substances, divalent cations, and Fe have been observed in acid sulfate environments, where dissolved Fe mobility is effectively reduced through complexation and sorption mechanisms (Shahabi-Ghahfarokhi et al., 2022). Furthermore, Sarangi et al. (2022) highlighted that organic complex-mediated stabilization of Fe limits acidification feedbacks driven by Fe oxidation, which aligns with the mitigation effects observed under nano-zeolite and C-humate treatments in this study.

Based on the results and discussion above, a proposed mechanism for adsorption or cation exchange that occurs on the surface of nanozeolites and humic compounds can be formulated as illustrated in Figure 5. The proposed mechanisms illustrated in Figure 5 accurately describe the interfacial reactions occurring between nano-zeolite, Ca-humate, and dissolved ions in acid sulfate soils. On the nano-zeolite surface, the dominant process involves specific ion exchange at negatively charged siloxane sites (≡Si–O^-), where Ca^{2+} and K^+ initially bound to the zeolite framework are released into the soil solution and selectively replaced by high-charge metal cations such as Fe^{3+} and Al^{3+}. This mechanism, represented by Reaction (1), results in the strong immobilization of these toxic metal ions via inner-sphere complexation, providing a thermodynamically stable retention mechanism. Simultaneously, the role of Ca-humate is well supported by Reaction (2), which operates through a dual complexation and ion-replacement mechanism: Ca^{2+} coordinated to carboxyl groups forms cation-bridging complexes with sulfate (SO_4^{2-}), thereby lowering sulfate activity, while Ca^{2+} loosely bound to phenolic groups is preferentially replaced by Fe^{3+} following HSAB principles, leading to the formation of stable Fe-humate complexes and the release of Ca^{2+} back into the soil solution. Together, these reactions provide a coherent explanation for the observed reductions in Fe^{3+}, Al^{3+}, and SO_4^{2-} concentrations in the soil solution, highlighting the complementary roles of nano-zeolite and Ca-humate in improving the chemical quality of acid sulfate soils.

Consistent with these mechanisms, the statistical results of this study demonstrated significant negative correlations between soil pH and soluble Fe and Al, and a positive association between available Ca and the reductions in these metal species, confirming the critical importance of pH-driven Fe/Al immobilization and Ca-mediated stabilization pathways. The decline in SO_4^{2-} availability with increasing humate binding capacity further supports the involvement of cation bridging and organo-mineral complexation processes.

This study provides the first integrated evidence that coupling nano-zeolite with Ca-humate simultaneously modifies cation and anion geochemistry through coordinated ion exchange and ligand complexation in acid sulfate soils. The demonstrated dual-mechanism approach offers a more effective remediation strategy than single-amendment applications, advancing current understanding of interfacial geochemical controls on Fe, Al, and SO_4^{2-} dynamics in highly acidic soil environments

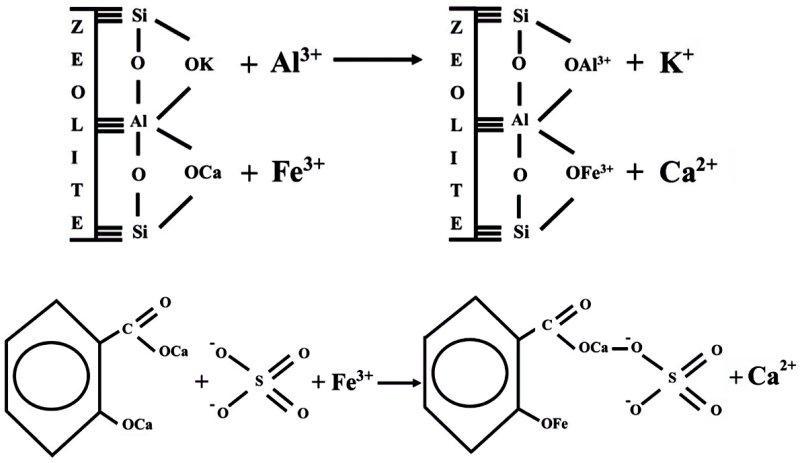

Figure 5. Proposed reaction mechanism of nano-zeolite and Ca-humat in altering the chemical quality of acid sulfate soil from Segoro Anakan, Cilacap, Central Java

CONCLUSIONS

The combined application of nano-zeolite (12 t ha^{-1}) and Ca-humate (10.32 t ha^{-1}) proved highly effective in improving the chemical properties of acid sulfate soils. This treatment reduced the solubility of Al^{3+}, Fe^{2+}, SO_4^{2-}, and pyrite by 59.5%, 42.7%, 79.2%, and 50%, respectively, while simultaneously enhancing the availability of Ca^{2+}, Mg^{2+}, K^+, and Na^+ by 33.4%, 14%, 72.2%, and 65.3%. These effects are primarily attributed to ion exchange between Al^{3+}/Fe^{3+} and base cations (Ca^{2+}, K^+, Na^+) within the nano-zeolite structure, as well as complexation reactions between Ca-humate and metal ions through carboxylic and phenolic functional groups. The overall mechanism results in reduced exchangeable acidity, enhanced soil buffering capacity, and improved macronutrient availability. The complementary and partially synergistic interactions of nano-zeolite and Ca-humate thus represent a viable and sustainable amelioration strategy for mitigating Al and Fe toxicity in tropical acid sulfate soils, particularly within coastal reclamation and agricultural development programs.

Acknowledgements

We would like to express our gratitude to Universitas Gadjah Mada for providing funding to carry out this research.

REFERENCES

1. Aainaa, H.N, Ahmed, O. H., Ab Majid, N. M. (2018). Effects of clinoptilolite zeolite on phosphorus dynamics and yield of Zea mays L. cultivated on an acid soil. *PLOS ONE, 13*(9), e0204401. https://doi.org/10.1371/journal.pone.0204401
2. Adila, Z., Trisunaryanti, W., Triyono, T. (2024). Modification of natural zeolite from Klaten, indonesia using ammonium chloride by ion-exchange and its application as catalyst in ethanol dehydration to produce diethyl ether. *Indonesia. J. Chem., 24*(2), 505–518. https://jurnal.ugm.ac.id/ijc/article/view/90279/38527
3. Antu, U.B., Roy, T.K., Kulsum, T.I., Mitu, P.R., Ismail, Z., Arifin, M., Datta, M., Hossain, S.A., Islam, M.S., Mahiddin, N.A., Al Bakky, A., Hossin, S., Islam, S., M.Idris, A. (2025). Role of humic acid for climate change adaptation measures to boost up sustainable agriculture and soil health: A potential review, *International Journal of Biological Macromolecules, 313*, 144043. https://doi.org/10.1016/j.ijbiomac.2025.144043
4. Ardli, E.R., Yani, E. (2020). Mangrove Damage Evaluation using Two Species of Acanthus as a Biomonitoring Agent, Case Study: Segara Anakan Cilacap, Indonesia. *IOP Conf. Series: Earth and Environmental Science 550*, 012001. IOP Publishing https://doi.org/10.1088/1755-1315/550/1/012001
5. Ardli, E.R., Yuwono, E., Purwanto, A.D. (2022). Land cover changes and impacts of massive siltation on the mangrove Segara Anakan Lagoon system, Cilacap Indonesia. *Journal of Ecological Engineering, 23*(7), 29–41. https://doi.org/10.12911/22998993/149821
6. Ardli, E. R., Wolff, M. (2009). Land use and land cover change affecting habitat distribution in the Segara Anakan Lagoon, Indonesia. Regional Environmental Change, 9(4), 235–243. https://doi.org/10.1007/s10113-008-0072-6
7. Astuti, D.W., Mudasir, Aprilita, N.H. (2019). Preparation and characterization adsorbent based on zeolite from Klaten, Central Java, Indonesia. *Journal of Physics: Conference Series 1156,* 012002. https://doi.org/10.1088/1742-6596/1156/1/012002
8. Azman, E. A., Ismail, R., Ninomiya, S., Jusop, S., Tongkaemkaew, U. (2023). The effect of calcium silicate and ground magnesium limestone (GML) on the chemical characteristics of acid sulfate soil. *PLOS ONE, 18*(9), e0290703. https://doi.org/10.1371/journal.pone.0290703
9. Bautista, I., Oliver, J., Lidón, A., Osca, J. M., Sanjuán, N. (2023). Improving the chemical properties of acid sulphate soils from the Casamance River Basin. *Land, 12*(9), 1693. https://doi.org/10.3390/land12091693
10. Belviso, C. (2020). Zeolite for potential toxic metal uptake from contaminated soil: A brief review. *Processes, 8*(7), 820. https://doi.org/10.3390/pr8070820
11. Cahyo, T. N., Hartoko, A., Muskananfola, M. R., Haeruddin, Hilmi, E. (2024). Mangrove density and delta formation in Segara Anakan Lagoon as an impact of the riverine sedimentation rate. *Biodiversitas, 25*(3), 1276–1285. https://doi.org/10.13057/biodiv/d250344
12. Cataldo, D., Cacchio, P., De Marco, A. (2021). Zeolites in agriculture: a review of uses and potential environmental benefits. *Agronomy, 11*(8), 1547. https://doi.org/10.3390/agronomy11081547
13. Christanto, J. (2009). The Environmental management of the Segara Anakan Lagoon and its surroundings, Cilacap, Central Java, Indonesia. *Geomedia Majalah Ilmiah dan Informasi Kegeografian, 7*(2). https://doi.org/10.21831/gm.v7i2.19078
14. Deng, A., Wu, X., Su, C., Zhao, M., Wu, B., Luo, J. (2021). Enhancement of soil microstructural

stability and alleviation of aluminium toxicity in acidic latosols via alkaline humic acid fertiliser amendment. *Chemical Geology, 583*, 120473. https://doi.org/10.1016/j.chemgeo.2021.120473.

15. Dhanya, K. R., Gladis, R. (2017). Acid sulfate soils – Its characteristics and nutrient dynamics. *An Asian Journal of Soil Science, 12*(1), 221–227. https://doi.org/10.15740/HAS/AJSS/12.1/221-227
16. Doni, S., Masciandaro, G., Macci, C., Manzi, D., Mattii, G. B., Cataldo, E., Gispert, M., Vannucchi, F., Peruzzi, E. (2024). Zeolite and winery waste as innovative by-product for vineyard soil management. *Environments, 11*(2), 29. https://doi.org/10.3390/environments11020029
17. Dyer, A. (2005). Ion-exchange properties of zeolites. *Studies in Surface Science and Catalysis, 157*, 181–204. https://doi.org/10.1016/S0167-2991(05)80011-4
18. Estiaty, L. M. (2015). Synthesis and characterization of zeolite-TiO_2 from modified natural zeolite. *Journal of Coal and Mineral Technology, 11*(3), 181–190. (in Indonesia).
19. https://jurnal.tekmira.esdm.go.id/index.php/minerba/article/view/721/563
20. Eviati, S., Herawaty, L., Anggria, L., Usman, Tantika, H.E., Prihatini, R., Wuningrum, P. (2023). Chemical analysis of soil, plants, water, and fertilizer. *Soil and Fertilizer Instrument Standard Testing Center, Ministry of Agriculture, Indonesia* (in Indonesia).
21. Fitzpatrick, R. W., Powell, B., Marvanek, S. (2008). *Atlas of Australian Acid Sulfate Soils.* In Inland Acid Sulfate Soil Systems Across Australia (Eds Rob Fitzpatrick and Paul Shand). 75–89. CRC LEME Open File Report No. 249. Perth, Australia.
22. Fitzpatrick, R. W., Shand, P., Mosley, L. M. (2017). Acid sulphate soil evolution models and pedogenic pathways during drought and reflooding cycles in irrigated areas and adjacent natural wetlands. *Geoderma, 308*, 270–290. https://doi.org/10.1016/j.geoderma.2017.08.016
23. Gillespie, C. J., Antonangelo, J. A., Zhang, H. (2021). The response of soil pH and exchangeable Al to alum and lime amendments. *Agriculture, 11*(6), 547. https://doi.org/10.3390/agriculture11060547
24. Hasbullah, N. A., Ahmed, O. H., Majid, N. M. A. (2020). Effects of amending phosphatic fertilizers with clinoptilolite zeolite on phosphorus availability and its fractionation in an acid soil. *Applied Sciences, 10*(9), 3162. https://doi.org/10.3390/app10093162
25. Hilmi, E., Amron, Sari, L.K., Cahyo, T.N., Siregar, A.S. (2021). The mangrove landscape and zonation following soil properties and water inundation distribution in Segara Anakan Cilacap. *Jurnal Manajemen Hutan Tropika, 27*(3), 152–164. https://journal.ipb.ac.id/jmht/article/view/33333/22506
26. Hriciková, S., Kožárová, I., Hudáková, N., Reitznerová, A., Nagy, J., Marcinčák, S. (2023). Humic substances as a versatile intermediary. *Life, 13*(4), 858. https://doi.org/10.3390/life13040858
27. Igathinathane, C., Pordesimo, L.O., Columbus, E.P., Batchelor, W.D., Methuku, S.R. (2008). Shape identification and particles size distribution from basic shape parameters using ImageJ. *Computers and Electronics in Agriculture, 63*(2), 168–182. https://doi.org/10.1016/j.compag.2008.02.007
28. Inglezakis, V. J., Zorpas, A. A. (Eds.). (2012). *Handbook of Natural Zeolites.* Bentham Science Publishers. https://doi.org/10.2174/97816080526151120101
29. Jarosz, R., Szerement, J., Gondek, K., Mierzwa-Hersztek, M. (2022). The use of zeolites as an addition to fertilisers – A review. *Catena, 213*, 106125. https://doi.org/10.1016/j.catena.2022.106125
30. Javaid, A., Munir, N., Abideen, Z., Siddiqui, Z. S., Yong, J. W. H. (2024). The role of natural and synthetic zeolites as soil amendments for mitigating the negative impacts of abiotic stresses to improve agricultural resilience. *Plant Stress, 14*, 100627. https://doi.org/10.1016/j.stress.2024.100627
31. Johnston, S. G., Morgan, B., Burton, E. D. (2016). Legacy impacts of acid sulfate soil runoff on mangrove sediments: reactive iron accumulation, altered sulfur cycling and trace metal enrichment. *Chemical Geology,* 427–428, 43–53. https://doi.org/10.1016/j.chemgeo.2016.02.013
32. Khan, I., Saeed, K., Khan, I. (2017). Nanoparticles: Properties, applications, and toxicities. *Arabian Journal of Chemistry, 12*(7), 908–931. https://doi.org/10.1016/j.arabjc.2017.05.011
33. Khan, M.Z.h., Islam, M.R., Nahar, N., Al-Mamun, M.R., Khan, M.A.S., Matin, M.A. (2021). Synthesis and characterization of nanozeolite-based composite fertilizer for sustainable release and use efficiency of nutrients. *Heliyon, 7*(1), e06091. https://doi.org/10.1016/j.heliyon.2021.e06091
34. Kordala, N., Wyszkowski, M. (2024). Zeolite properties, methods of synthesis, and selected applications. *Molecules, 29*, 1069. https://doi.org/10.3390/molecules29051069
35. Kumalasari, R., Hanudin, E., Nurudin, M. (2021). *Effectiveness of NK Fertilizer Coated with Nano Zeolite and Crab Shells on Shallots in Entisol and Inceptisol Soil. Thesis (in Indonesia).* Department of Soil Sciences, Faculty of Agriculture, Universitas Gadjah Mada, Yogyakarta, Indonesia. https://etd.repository.ugm.ac.id/penelitian/detail/206658
36. Kumalasari, R., Hanudin, E., Nurudin, M. (2022). Increasing growth and yield of shallot using nano zeolite and nano crab shell encapsulated NK fertilizer in entisols and inceptisols. *Planta Tropika: Jurnal Agrosains (Journal of Agro Science), 10*(2), 140–151. https://journal.umy.ac.id/pt/article/view/12945

37. Kuznetsov, P., Malyavin, V., Dement'ev, K. (2025). Insights into ball milling for the production of highly active zeolites for catalytic cracking of VGO. *Catalysts, 15*(6), 596. https://doi.org/10.3390/catal15060596
38. Latifah, O., Ahmed, O. H., Majid, N. M. A. (2017). Enhancing nitrogen availability from urea using clinoptilolite zeolite. *Geoderma, 306*, 152–159. https://doi.org/10.1016/j.geoderma.2017.07.012
39. Lațo, A., Berbecea, A., Lațo, I., Crista, F., Crista, L., Sala, F., Radulov, I. (2025). Mitigating soil acidity: Impact of aglime ($CaCO_3$) particle size and application rate on exchangeable aluminium and base cations dynamics. *Sustainability, 17*(18), 8135. https://doi.org/10.3390/su17188135
40. Legese, W., Taddesse, A. M., Kibret, K., Wogi, L. (2024). Effects of natural and modified zeolite based composite fertilizers on slow release and nutrient use efficiency. *Heliyon, 10*(3), e25524. https://doi.org/10.1016/j.heliyon.2024.e25524
41. Li, Y., Fang, F., Wei, J., Wu, X., Cui, R., Li, G., Zheng, F., Tan, D. (2019). Humic acid fertilizer improved soil properties and soil microbial diversity of continuous cropping peanut: a three-year experiment. *Scientific Reports, 9*, 12014. https://www.nature.com/articles/s41598-019-48620-4
42. Li, R., Guo, X., Qi, Y., Wang, Y., Wang, J., Zhang, P., Cheng, S., He, W., Zhao T., Li, Y., Li, L., Ji, J., He, A., Ai, Z. (2025). Soil amendments and slow-release urea improved growth, physiological characteristics, and yield of salt-tolerant rice under salt stress conditions. *Plants, 14*(4), 543. https://doi.org/10.3390/plants14040543
43. Lima, D. S. D., Zapelini, I. W., Silva, L. L., Mintova, S., Martins, L. (2024). Impacts of ball-milling on ZSM-5 zeolite properties and its catalytic activity in the two-phase glycerol ketalization with acetone. *Catalysis Today, 441*, 114842. https://doi.org/10.1016/j.cattod.2024.114842
44. Maffia, A., Oliva, M., Marra, F., Mallamaci, C., Nardi, S., Muscolo, A. (2025). Humic substances: Bridging ecology and agriculture for a greener future. *Agronomy, 15*(2), 410. https://doi.org/10.3390/agronomy15020410
45. Maftu'ah, E., Saleh, M., Sulaeman, Y., Napisah, K., Agustina, R., Mukhlis, M., Anwar, K., Ningsih, R.D., Masganti, M., Maharani, P.H., Asikin, S., Karolinoerita, V., Wakhid, N., Hayati, A., Lestari, Y. (2024). Si-humate as soil ameliorant to improve the properties of acid sulfate soil, growth, and rice yield. *Chilean Journal of Agricultural Research, 84*(2), 267–280. https://oes.chileanjar.cl/files/CJAR230356-84-2-2024.pdf
46. Maharani, P. H., Maftu'ah, E., Sulaeman, Y., Napisah, K., Masganti, M., Mukhlis, M., Anwar, K., Ningsih, R. D., Chairuman, N. (2025). Integrated rice husk biochar and compost to improve acid sulfate soil properties and corn growth. *Journal of Degraded and Mining Lands Management, 12*(4), 8097–8106. https://doi.org/10.15243/jdmlm.2025.124.8097
47. Martínez, J.M., Galantini, J.A., Duval, M.E., López, F.M., Iglesias, J.O. (2018). Estimating soil organic carbon in Mollisols and its particle-size fractions by loss-on-ignition in the semiarid and semihumid Argentinean Pampas. *Geoderma Regional, 12*, 49–55. https://doi.org/10.1016/j.geodrs.2017.12.004
48. Mondal, M., Benukar, B., Sourav, G., Sukamal, S., Hirak, B., Koushik, B., Kumar, B.P., Sagar, M., Marian, B., Milan, S., Peter, O., Hossain, A. (2021). Zeolites enhance soil health, crop productivity, and environmental safety. *Agronomy, 11*(3), 448. https://doi.org/10.3390/agronomy11030448
49. Nassrullah, H., Anis, S. F., Lalia, B. S., Hashaikeh, R. (2022). Cellulose nanofibrils as a damping material for the production of highly crystalline nanosized zeolite Y via ball milling. *Materials, 15*(6), 2258. https://doi.org/10.3390/ma15062258
50. Omar, L., Ahmed, O. H., Jalloh, M. B., Nik Muhamad, A. M. (2020). Soil nitrogen fractions, nitrogen use efficiency and yield of *Zea mays* L. grown on a tropical acid soil treated with composts and clinoptilolite zeolite. *Applied Sciences, 10*(12), 4139. https://doi.org/10.3390/app10124139
51. Palansooriya, K. N., Shaheen, S. M., Chen, S. S., Tsang, D. C. W., Hashimoto, Y., Hou, D., Bolan, N. S., Rinklebe, J., Ok, Y. S. (2020). Soil amendments for immobilization of potentially toxic elements in contaminated soils: A critical review. *Environment International, 134*, Article 105046. https://doi.org/10.1016/j.envint.2019.105046
52. Pansu, M., Gautheyrou, J. (2006). *Handbook of Soil Analysis: Mineralogical, Organic and Inorganic Methods.* Springer-Verlag Berlin Heidelberg, The Netherlands.
53. Reddy, K. R., DeLaune, R. D., Inglett, P.W. (2023). *Biogeochemistry of wetlands: Science and applications. 2nd edition, CRC Press.* Taylor & Francis Group, London.
54. Rosalina, H. (2016). Development of alternatives to mitigate deterioration of Segara Anakan Lagoon as revealed by analytical hierarchy process (AHP). *Journal of the Civil Engineering Forum, 2*(3). https://doi.org/10.22146/jcef.26587
55. Sabang, R., Nurjanna, Pasande, R. (2005). Pyrite analysis in acid sulfate soil ponds. *Buletin Teknik Litkayasa Aquakultur, 4*(2), 37–41 (in Indonesia).
56. Sanchez, P. A. (2019). *Properties and management of soils in the tropics (2nd ed.).* Cambridge University Press.
57. Santi, M. A., Somboon, S., Thip-Amat, S., Sukitprapanon, T. S., Lawongsa, P. (2024). Effects of

humic acid application on bacterial diversity under maize cultivation. *Agrosystems, Geosciences & Environment, 7*(3), e20547. https://doi.org/10.1002/agg2.20547

58. Sarangi, S.K., Mainuddin, M., Maji, B. (2022). Problems, management, and prospects of acid sulphate soils in the Ganges delta. *Soil System, 6*, 95. https://doi.org/10.3390/soilsystems6040095
59. Sari, L. K., Adrianto, L., Soewardi, K., Atmadipoera, A. S., Hilmi, E. (2016). Sedimentation in Lagoon Waters (Case Study on Segara Anakan Lagoon). The 5th International Symposium on Earthhazards and Disaster Mitigation. *AIP Conference Proceedings*. https://doi.org/10.1063/1.4947417
60. Senilă, M., Cadar, O. (2024). Modification of natural zeolites and their applications for heavy metal removal from polluted environments: Challenges, recent advances, and perspectives. *Heliyon, 10*(3), e25303. https://doi.org/10.1016/j.heliyon.2024.e25303
61. Shamshuddin, J., Elisa Azura, A., Shazana, M.A.R.S., Fauziah, C.I., Panhwar, Q.A., Naher, U.A. (2014). Properties and management of acid sulfate soils in Southeast Asia for sustainable cultivation of rice, oil palm, and cocoa. *Advances in Agronomy, 124*, 91–142. https://doi.org/10.1016/B978-0-12-800138-7.00003-6
62. Shahabi-Ghahfarokhi, S., Rahmati-Abkenar, M., Matson, J. G., Karimi, H., Yu, C., Hogland, W., Klavinš, M., Ketzer, M. (2022). Removal and potential recovery of dissolved metals from acid sulfate soil drainage by spent coffee-grounds and dissolved organic carbon. *Environmental Advances, 8*, 100193. https://doi.org/10.1016/j.envadv.2022.100193
63. Sharma, V., Javed, B., Byrne, H., Curtin, J., Tian, F. (2022). Zeolites as carriers of nano-fertilizers: from structures and principles to prospects and challenges. *Applied Nano 3*, 163–186. https://www.mdpi.com/2673-3501/3/3/13
64. Sipos, P., Kovács Kis, V., Balázs, R., Tóth, A., Németh, T. (2021). Effect of pedogenic iron-oxyhydroxide removal on the metal sorption by soil clay minerals. *Journal of Soils and Sediments, 21*, 1785–1799. https://doi.org/10.1007/s11368-021-02899-x
65. Subramanian, K. S., Manikandan, A., Thirunavukkarasu, M., Rahale, C. S. (2015). *Nano-fertilizers for Balanced Crop Nutrition.* Nanotechnologies in Food and Agriculture 69–80. Springer International Publishing. https://doi.org/10.1007/978-3-319-14024-7_3
66. Sulaeman, Y., Maftuáh, E., Noor, M., Hairani, A., Nurzakiah, S., Mukhlis, M., Ningsih, R. D. (2024). Coastal acid-sulfate soils of kalimantan, indonesia, for food security: characteristics, management and future directions. *Resources, 13*(3), 36. https://doi.org/10.3390/resources13030036
67. Thirunavukkarasu, M., Subramanian, K. S. (2014). Surface modified nano-zeolite used as a carrier for slow release of sulphur. *Journal of Applied and Natural Science 6(1), 19–26*. https://doi.org/10.31018/jans.v6i1.369
68. Wang, X., Wang, J., Yan, P., Zuo, Q., Sun, Q., Liu, D. (2025). Organic fertilizer in combination with zeolite enhanced maize yield with lower greenhouse gas emissions in sandy loam soil in North China. *Frontiers in Sustainable Food Systems, 9*, 1614139. https://doi.org/10.3389/fsufs.2025.1614139
69. Whitton, M.M., Ren, X., Yu, S.J., Irving, A.D., Trotter, T., Bajagai, Y.S., Stanley, D. (2023). Humate application alters microbiota–mineral interactions and assists in pasture dieback recovery. *Heliyon, 9*(2), e13327. https://doi.org/10.1016/j.heliyon.2023.e13327
70. Yin, N., Geng, N., Wang, T., Wang, H., Pan, H., Yang, Q., Lou, Y., Zhuge, Y. (2023). Effect of acidification on clay minerals and surface properties of brown soil. *Sustainability, 15*(1), 179. https://doi.org/10.3390/su15010179